The STIM-Orai Pathway 2

STIM/Orai Structures: Isolated and in Complex

Jinhui Zhu[a], Qingping Feng[a] and Peter B. Stathopulos [a*,1]

[a] Department of Physiology and Pharmacology, Schulich School of Medicine and Dentistry, Western University, London, Ontario, Canada
[1] Email: peter.stathopulos@schulich.uwo.ca

Abstract

Considerable progress has been made elucidating the molecular mechanisms of calcium (Ca^{2+}) sensing by stromal interaction molecules (STIMs) and the basis for Orai channel activity. This chapter focuses on the available high resolution structural details of STIM and Orai proteins with respect to the regulation of store operated Ca^{2+} entry (SOCE). Solution structures of the Ca^{2+} sensing domains of STIM1 and STIM2 are reviewed in detail, crystal structures of cytosolic coiled-coil STIM fragments are discussed and an overview of the closed *Drosophila melanogaster* Orai hexameric structure is provided. Additionally, we highlight structures of human Orai1 N-terminal and C-terminal domains in complex with calmodulin and human STIM1, respectively. Ultimately, the accessible structural data are discussed in terms of potential mechanisms of action and cohesiveness with functional observations.

2.1 Background

The calcium ion (Ca^{2+}) is a universal messenger which controls a vast number of cellular processes such as the prolonged regulation of transcription, cell division and apoptosis, as well as more short-lived secretion and contraction (Berridge et al. 2003; Berridge 2009; Bootman and Lipp 2001). The voltage-independent mode of store-dependent Ca^{2+} mobilization is conserved among eukaryotic cells: agonist-induced stimulation of G-protein-coupled, T-cell or tyrosine kinase receptors activate phospholipase C β or γ2, leading to the hydrolysis of membrane-associated phosphoinositide 4,5-bisphosphate, yielding inositol 1,4,5-trisphosphate (IP_3). IP_3 is a small diffusible second messenger which binds to the IP_3 receptor (IP_3R) on the ER membrane. Binding of IP_3 allosterically opens this Ca^{2+} release channel, thus allowing Ca^{2+} to move down the concentration gradient from the lumen into the cytoplasm. The endoplasmic reticulum (ER) lumen can only transiently supply the cytosol with Ca^{2+} before it is rapidly depleted. In excitable cells, ryanodine receptors (RyRs) play a larger role in sarcoplasmic reticulum (SR) luminal Ca^{2+} depletion than the IP_3Rs. After diminishment of ER/SR stored Ca^{2+}, highly Ca^{2+} selective and permeable store operated channels (SOC)s on the plasma membrane (PM) open, providing sustained Ca^{2+} influx into the cytosol from the virtually inexhaustible extracellular Ca^{2+} supply. Ultimately, the cytosolic influx of Ca^{2+} replenishes the luminal stores via the SR/ER Ca^{2+} ATPase pump. This specific

communicative interchange of Ca^{2+} between the ER/SR lumen, cytosol and extracellular space is termed store operated Ca^{2+} entry (SOCE).

Although SOCE was proposed over two decades ago (Putney 1986), the major molecular players were identified and began to be characterized ~20 years following the conceptualization of this model, with the stromal interaction molecules (STIMs) functioning as the ER/SR Ca^{2+} sensors and PM SOC activators (Liou et al. 2005; Roos et al. 2005; Zhang et al. 2005), and the Orai proteins serving as the major PM channel components (Feske et al. 2006; Prakriya et al. 2006; Vig et al. 2006a; Vig et al. 2006b; Yeromin et al. 2006; Zhang et al. 2006). Orai1-composed SOCs are termed Ca^{2+} release activated Ca^{2+} (CRAC) channels due to the voltage-independent, highly Ca^{2+} selective and inward-rectifying currents generated during activity which is distinct from other SOCs. SOCE via CRAC channels is the primary mode of augmenting cytosolic Ca^{2+} in lymphocyte signaling.

Human Orai1 is composed of 301 amino acids and has four transmembrane (TM) segments (Cai 2007; Feske 2007). Both the amino and carboxy termini of this PM protein reside in the cytoplasm and each has been implicated as a critical accessory region in Orai1 activation via direct and indirect interactions with STIM1 (Derler et al. 2013; Frischauf et al. 2009; McNally et al. 2013; Muik et al. 2008; Muik et al. 2012; Palty et al. 2015; Palty and Isacoff 2016; Park et al. 2009; Yuan et al. 2009; Zheng et al. 2013; Zhou et al. 2010a). Humans encode three homologues (i.e. Orai1, Orai2, Orai3) showing conservation in the predicted TM domains, acidic residues involved in ion permeability and selectivity, as well basic residue position associated with SCID. Transmission electron microscopy images of Orai1 suggest that Orai1 tetramers form a teardrop-shaped structure that extends into the cytosol sufficiently for direct interaction with STIM1 at ER-PM junctions (i.e. ~10 nm) (Maruyama et al. 2009). The TM1 segment constitutes the central pore of Orai channels (McNally et al. 2009; McNally and Prakriya 2012; McNally et al. 2012; Prakriya et al. 2006; Yeromin et al. 2006; Zhang et al. 2011; Zhou et al. 2010b); moreover, published data supports both tetrameric (Demuro et al. 2013; Maruyama et al. 2009; Mignen et al. 2008; Penna et al. 2008; Thompson and Shuttleworth 2013) and hexameric architectures (Balasuriya et al. 2014; Hou et al. 2012; Zhou et al. 2010b).

Upon ER Ca^{2+} store depletion, STIM1 moves from a pervasive ER distribution to distinct punctate aggregates at ER-PM junctions (Liou et al. 2005; Zhang et al. 2005). This cluster of Ca^{2+}-depleted STIM1 facilitates recruitment of Orai1 to the same junctions, establishing sites of open CRAC channels (Luik et al. 2006; Varnai et al. 2007; Wu et al. 2006; Xu et al. 2006). The present chapter focuses on a comparison of the high resolution structural properties of the Ca^{2+} sensing regions of human STIM1 and STIM2; further, the work discusses available crystal structure information on the cytosolic coiled-coil (CC) domains of STIM1 as well as *Drosophila melanogaster* Orai. In addition to this structural data of STIM and Orai fragments in isolation, the structural elucidations of the N- and C-terminal regions of Orai1 in complex with calmodulin (CaM) and a human STIM1 CC region, respectively are reviewed. Collectively, these high resolution structural details provide important insights into the mechanisms that activate and promote relocalization of STIMs to ER-PM junctions and the basis for STIM coupling with Orai subunits.

2.3 Stromal Interaction Molecule Domain Organization

Human STIM1 is a type I TM protein of 685 amino acids localized on ER/SR membranes or on the PM following post-translational *N*-glycosylation of Asn131 and Asn171 (Manji et al. 2000; Williams et al. 2001; Williams et al. 2002). Vertebrates encode a second homologue, STIM2, which contains regions highly conserved with STIM1 within both the luminal and cytosolic domains. Unlike STIM1, STIM2 does not appear to localize on the PM, despite conservation of the STIM1 Asn131 residue. The most homologous regions between STIM1 and STIM2 include the EF-hand, sterile α motif (SAM) domain as well as two cysteines within the luminal domains and three coiled-coil domains, a Lys-rich and a Pro/Ser-rich segment within the cytosolic region (Fig. 2.1A). Both proteins encode a single-pass TM region identifiable in hydropathy plots. ER localization of STIM1 is signaled through the first 22 amino acids. STIM2, on the other hand, encodes an additional 87 residues distally toward the N-terminus outside of the homologous ER signal peptide sequences. Early studies proposed that translation initiation of STIM2 occurs at a non-AUG site (Williams et al. 2001); however, more recently it has been suggested that the much longer signal sequence of STIM2, upstream of and including the homologous STIM1 signal peptide (i.e. residues 1 – 101) (Fig. 2.1B), is necessary for appropriate ER localization of STIM2 proteins (see Chap. 2.4) (Graham et al. 2011). Phosphorylation of various STIM1 Ser and Thr residues within the Ser/Pro-rich region has also been described (Pozo-Guisado et al. 2010; Smyth et al. 2009).

CRAC channel activation by ER-residing STIM1 is a multi-step process: first, STIM1 oligomerization on the ER membrane occurs in response to ER luminal Ca^{2+} depletion; second, STIM1 homotypic oligomers translocate to ER-PM junctions; third, CRAC channels composed of PM Orai1 subunits are recruited and open at these junctions (Liou et al. 2007). The cytosolic regions of STIMs play a role in the oligomerization of Ca^{2+}-depleted STIM1 (Covington et al. 2010; Muik et al. 2009), in targeting STIM1 to the ER-PM junctions and in mediating the interactions between STIM1 and Orai1 pore subunits (Baba et al. 2006; Huang et al. 2006; Li et al. 2007; Liou et al. 2007). Three separate investigations identified cytosolic STIM1 residues 233-450 (i.e. Orai1 activating small fragment, OASF) (Muik et al. 2009), 342-448 (Park et al. 2009) (i.e. CRAC activating domain, CAD) and 344-443 (Yuan et al. 2009) (i.e. STIM1-Orai1 activating region, SOAR) as critical amino acid stretches through the conserved CC domains for inducing Orai1 channel activation.

The essential role of STIM1 in the activation of CRAC channels is evident from inhibiting RNA studies which demonstrate a significant attenuation in CRAC entry after STIM1 knockdown (Liou et al. 2005; Roos et al. 2005) and from STIM1/Orai1 co-overexpression data which show very large augmentations in ER Ca^{2+}-depletion dependent SOCE (Mercer et al. 2006; Soboloff et al. 2006). Along with a role in SOCE, STIM2 more prominently controls basal Ca^{2+} homeostasis (Bird et al. 2009; Brandman et al. 2007). A fraction of STIM2 is coupled to Orai1 at resting ER Ca^{2+} levels, probably due to a somewhat lower affinity for Ca^{2+} (Brandman et al. 2007; Zheng et al. 2011). Both STIM1 and STIM2 are indispensable in CRAC-induced immune cell activation, though STIM2 knockout (-/-) affects SOCE in T-cells and fibroblasts to a lesser extent than $STIM1^{-/-}$ (Bird et al. 2009; Oh-hora and Rao 2008). While both homologues are expressed in a variety of cell types, a vital role for STIM2 has been emphasized in neuronal Ca^{2+} signaling (Berna-Erro et al. 2009).

The EF-hand and SAM domains located in the luminal region of STIMs are conserved

from roundworms to vertebrates (Collins and Meyer 2011; Stathopulos et al. 2009). In humans, the EF-hand together with the SAM domain (i.e. EF-SAM) exhibit greater than 85 % sequence similarity (Fig. 2.1B). Live cell studies demonstrate that EF-SAM provides the machinery necessary to sense changes in luminal Ca^{2+} levels. Specifically, disruption of Ca^{2+}-binding via mutations in the canonical EF-hand causes STIM1 to constitutively form puncta independent of ER Ca^{2+} levels (Liou et al. 2005; Mercer et al. 2006; Roos et al. 2005; Spassova et al. 2006). Furthermore, deleting the SAM domain from STIM1 abrogates the ability of the protein to form inducible puncta (Baba et al. 2006), and exchanging EF-SAM with a rapamycin-inducible oligomerization domain allows control of STIM1 puncta formation via rapamycin treatment, independent of ER Ca^{2+} levels (Luik et al. 2008). Finally, at resting ER Ca^{2+} concentrations, fluorescent protein-tagged STIM1 constructs engineered without the cytosolic domains exhibit very low intermolecular fluorescence resonance energy transfer (FRET) levels (i.e. consistent with non-interacting EF-SAM domains) that are largely augmented upon Ca^{2+}-store depletion (Covington et al. 2010). In addition to cell biology work, recombinant expression and isolation of STIM1 and STIM2 EF-SAM domains has been a valuable approach in garnering unambiguous biochemical and structural data on this critical Ca^{2+} sensing region.

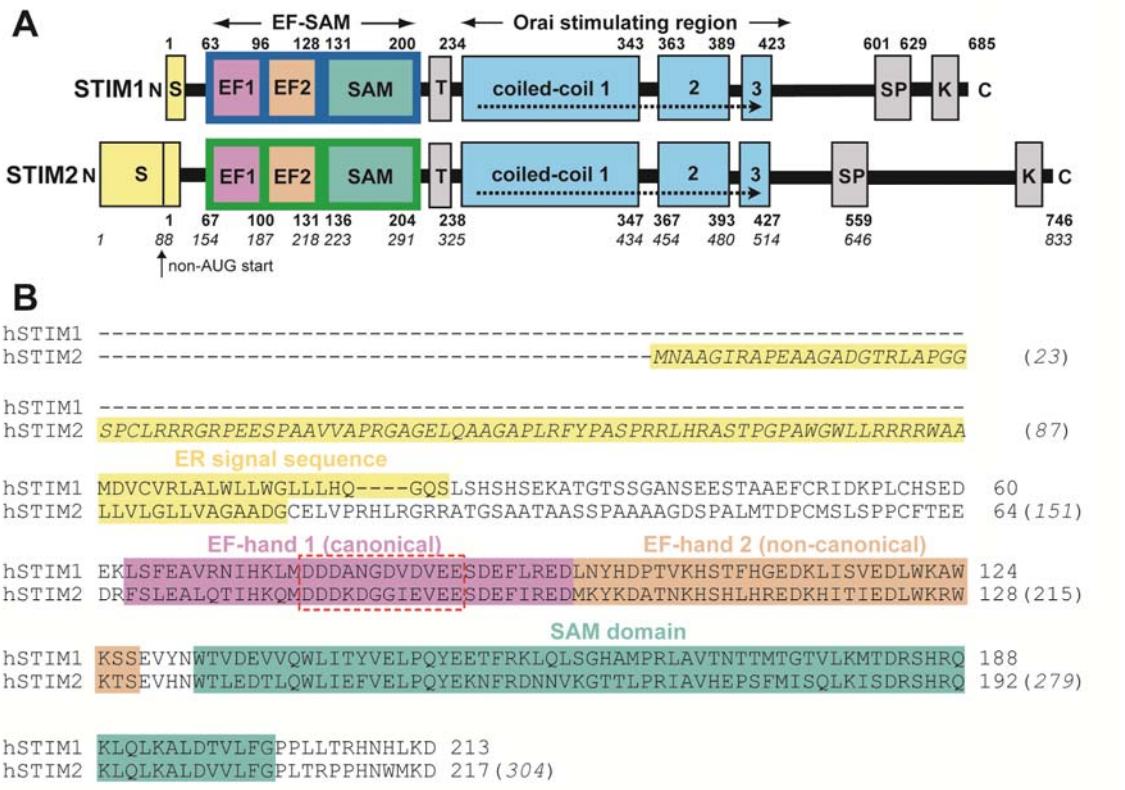

Fig.2.1 Primary sequence and domain architecture of STIM1 and STIM2. *A. Conserved domains in human STIM1 and STIM2.* Upstream of the signal peptides, S (yellow), the luminal domains include the canonical EF-hand, EF1 (violet), the non-canonical EF-hand, EF2 (beige), and the SAM domain (green). A single transmembrane pass, T, separates the cytosolic portion that include three putative coiled-coil domains (blue), a serine/proline-rich region, SP, and a lysine-rich (i.e. polybasic) region, K. Residue boundaries are indicated above and below STIM1 and STIM2, respectively. STIM2 contains a second set of numbering

(italics) corresponding to the entire STIM2 open reading frame. *B. Sequence conservation between human STIM1 and STIM2 luminal regions.* Amino acids through the domain boundaries are coloured as described in A. The canonical EF-hand loop residues involved in Ca^{2+} coordination are bounded by a box (red, broken lines). Residues shown in italics are upstream of the non-AUG start site for STIM2. Alignment was performed using ClustalW (Larkin et al. 2007).

2.4 Folding and Ca^{2+} Sensitivity of Isolated EF-SAM Domains

Throughout nature, EF-hands are found as pairs of helix-loop-helix motifs comprising single domains, and these EF-hand domains are fully capable of self-folding and cation binding. Similarly, SAM domains have been purified and characterized, folding into compact five-helix bundles, often showing a tendency for intermolecular association. The identification of STIMs as important regulators of CRAC entry inspired the recombinant expression, purification and characterization of these domains, in cis, on the same polypeptide chain, as they occur in STIMs. Remarkably, recombinant STIM1 EF-SAM unfolds through a single, highly cooperative transition using temperature or chemical denaturation (Stathopulos et al. 2006). Similarly, a single and cooperative transition is observed for STIM2 EF-SAM (Zheng et al. 2008), suggesting that the EF-hand and SAM domains of STIMs are co-dependent in overall stability and folding (Fig. 2.2A). The Ca^{2+}-depleted forms (i.e. apo) of STIM1 and STIM2 EF-SAM are markedly less stable than the Ca^{2+}-loaded counterparts (i.e. holo), but also exhibit single, cooperative unfolding curves. The temperature midpoint of unfolding (i.e. T_m) in single transition unfolding curves is a good indicator of protein stability. Apo STIM1 EF-SAM shows a T_m of ~19 ˚C compared to holo STIM1 EF-SAM with a T_m of ~45 ˚C near physiological pH (Stathopulos et al. 2006). The holo and apo states of STIM2 EF-SAM are more stable than STIM1 with T_m values of ~50 and 36 ˚C, respectively (Fig. 2.2A) (Zheng et al. 2008).

In the case of STIM1 EF-SAM, the protein undergoes a conformational change from a highly α-helical state in the presence of Ca^{2+} to a less well-folded state in the absence of Ca^{2+} (Fig. 2.2B). STIM2 EF-SAM also loses α -helicity in response to Ca^{2+} depletion; however, the structural transition is less striking, with apo STIM2 EF-SAM retaining considerable α -helicity (Fig. 2.2B) (Zheng et al. 2008). The ability of STIM2 EF-SAM to preserve a high degree of α -helicity in the absence of Ca^{2+} is consistent with the lesser destabilization observed in temperature denaturation experiments.

Consistent with the presence of a single canonical binding loop, STIM1 EF-SAM becomes saturated with Ca^{2+} at a molar ratio of ~1. The equilibrium dissociation constant (i.e. K_d), indirectly calculated using Ca^{2+}-induced changes in tertiary via intrinsic aromatic fluorescence or changes in secondary structure via far-UV circular dichroism, as well as directly measured via $^{45}Ca^{2+}$ titration is high (i.e. K_d between ~0.2 – 0.6 mM) compared to most vertebrate EF-hand proteins (Fig. 2.2C) (Stathopulos et al. 2006). The K_d of Ca^{2+} binding for STIM1 is temperature-dependent, with higher affinities (i.e. lower K_d) at lower temperatures. There is a high preference of the EF-hand for Ca^{2+} over Mg^{2+} since inclusion of Mg^{2+} in the experiments does not alter the binding curves. Grafting of the canonically defined EF-hand motif onto a stabilizing CD2 domain, and solution nuclear magnetic resonance (NMR) titration with Ca^{2+} shows a K_d of ~ 0.5 mM for the STIM1 EF-hand motif in pseudo-isolation (Huang et al. 2009). Considering the high sequence similarity between the STIM1 and STIM2 canonical EF-hand binding loops, it

is not surprising that STIM2 EF-SAM also exhibits a low affinity for Ca^{2+} in the same range as that determined for STIM1 (Fig. 2.2C). Nonetheless, it is important to note that similar probes of Ca^{2+} binding (i.e. fluorescence, CD, $^{45}Ca^{2+}$) applied to the STIM2 EF-SAM system produced considerably higher variability in the curves. This increased error and uncertainty is probably due to a somewhat lower Ca^{2+} affinity, albeit in the same sub-mM K_d range.

The inherent low affinity Ca^{2+} binding EF-hand motifs of STIMs are well suited to the relatively high Ca^{2+} levels in the ER/SR lumen. In resting, non-excitable cells, the ER luminal Ca^{2+} level is typically between 0.6 – 0.8 mM (Berridge et al. 2000; Berridge et al. 2003). Following agonist-induced stimulation, the luminal Ca^{2+} level may decrease, at least locally, to ~0.2 – 0.4 mM; moreover, with a Ca^{2+} binding K_d of ~0.2 – 0.6 mM, STIM1 has evolved to proficiently equilibrate between the Ca^{2+}-loaded and -free states in response to these fluctuations in ER Ca^{2+}. The *in vitro* Ca^{2+} binding data for STIM2, at least qualitatively, suggest a decreased affinity compared to STIM1 (Fig. 2.2C). Consistent with this *in vitro* work, full-length STIM2 forms puncta in response to smaller decreases in ER Ca^{2+} (i.e. at higher ER Ca^{2+} levels) compared to STIM1 (Bird et al. 2009; Brandman et al. 2007). This Ca^{2+} binding property of STIM2 facilitates a role for the ER-localized protein in regulating basal Ca^{2+} homeostasis, since at resting ER Ca^{2+} concentrations, a significant fraction of STIM2 may be Ca^{2+}-depleted and coupled to Orai1. Contributory to the Ca^{2+} store-independent regulatory mode of STIM2, may be cytosolic STIM2 that is not anchored to the ER membrane (Graham et al. 2011). In the cytosol, the vast majority of STIM2 molecules would be maintained in a Ca^{2+}-depleted state due to a Ca^{2+} level that is several orders of magnitude lower than the ER lumen (Feske 2007).

Homotypic oligomerization of STIM proteins following ER luminal Ca^{2+} depletion is a vital initiation step in the activation of SOCE (Liou et al. 2007; Stathopulos et al. 2006). In excess Ca^{2+} concentrations, STIM1 EF-SAM strictly exists as a monomer at physiological-like pH and temperatures below the thermal unfolding transition (Fig. 2.2D). In concert with the marked destabilization and partial unfolding accompanying Ca^{2+} depletion, STIM1 EF-SAM undergoes a change in quaternary structure, forming dimers and oligomers at low (i.e. 4 ˚C) and ambient temperatures (Stathopulos et al. 2006). On the other hand, STIM2 EF-SAM exhibits a resistance to oligomerization at low temperature, despite undergoing Ca^{2+}-depletion-induced destabilization, as observed for STIM1 (Fig. 2.2D) (Zheng et al. 2008). At ambient temperature, however, STIM2 EF-SAM oligomerizes, albeit with distinct kinetics compared to STIM1 EF-SAM (Stathopulos et al. 2009).

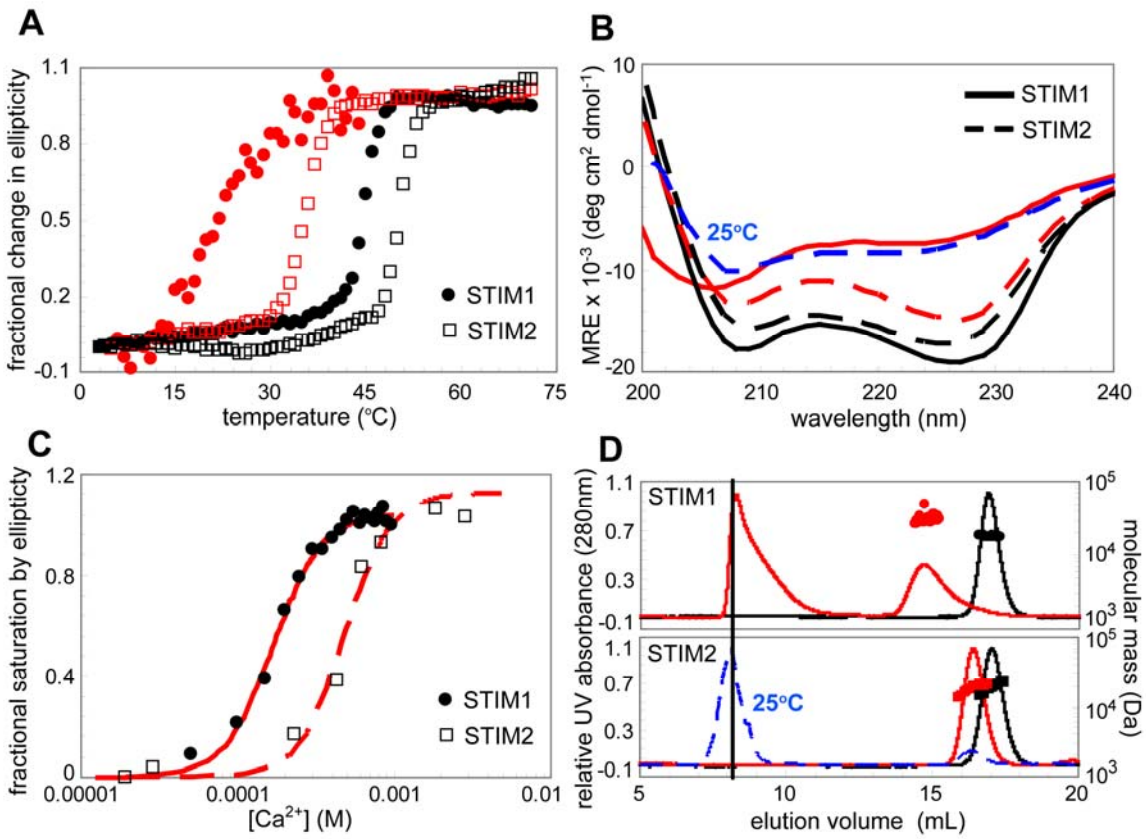

Fig. 2.2 *In vitro* Ca^{2+} sensing characteristics of STIM1 and STIM2 EF-SAM. *A. Thermal stability of EF-SAM proteins.* The change in far-UV CD at 225 nm is plotted as a function of temperature. Proteins in the presence of excess Ca^{2+} (i.e. holo) are plotted with black symbols and proteins in the absence of Ca^{2+} (i.e. apo) are plotted with red symbols. Circles and squares represent STIM1 and STIM2 EF-SAM, respectively [adapted from (Stathopulos et al. 2006; Zheng et al. 2008)]. *B. Secondary structure of EF-SAM proteins.* The far-UV CD spectra of holo and apo STIM1 are shown as solid black and red lines, respectively. The CD spectra of holo and apo STIM2 are shown as broken black and red lines, respectively. Apo STIM2 only exhibits a spectrum resembling apo STIM1 EF-SAM at 25 ˚C, shown as a broken blue line [adapted from (Stathopulos et al. 2006; Zheng et al. 2008)]. *C. Ca^{2+} binding to EF-SAM proteins.* Binding to STIM1 EF-SAM monitored by the fractional increase in negative ellipticity at 222 nm is plotted in circles. Binding to STIM2 EF-SAM is plotted in squares. The Hill equation fitted lines are shown in solid and broken red lines for STIM1 and STIM2, respectively. [Adapted from (Zheng et al. 2011)]. *D. Quaternary structure of EF-SAM proteins.* The STIM1 EF-SAM elution profiles in the presence (black line) and absence (red line) of Ca^{2+} are shown (upper panel). The MALS-determined monomeric molecular weight of holo and the dimeric molecular weight of apo STIM1 EF-SAM are shown above the elution peaks. The STIM2 EF-SAM elution profile in the presence (black line) and absence (red line) of Ca^{2+} is shown (lower panel). The MALS-determined monomeric molecular weights for holo and apo STIM2 EF-SAM at 4 ˚C are shown above the corresponding elution peaks. The 25 ˚C elution profile of apo STIM2 EF-SAM is shown as a broken blue line. The vertical black line intersects the S200 void volume showing that only apo STIM1 and STIM2 EF-SAM access the oligomerized state [adapted from (Stathopulos et al. 2006; Zheng et al. 2008)].

2.5 STIM1 and STIM2 EF-SAM Structure

NMR spectroscopy has been an invaluable tool for teasing out the precise atomic basis for the differences in the physicochemical properties between STIM1 and STIM2 EF-SAM. The Ca^{2+}-loaded form of STIM1 EF-SAM folds into a compact 10-helix structure

(Fig. 2.3A, left panel) (Stathopulos et al. 2008). A second EF-hand, not identified in the primary sequence of STIM1, is adjacent to the canonical EF-hand, stabilizing the Ca^{2+}-binding loop through hydrogen (H)-bonding. This H-bonding between the canonical and non-canonical EF-hand loops forms a short β-sheet. The three dimensional (3D) structure also exposes a short α -helix which links the EF-hand pair to the five-helix bundle SAM domain. Overall, the majority of the compact structure exhibits an acidic surface charge at neutral pH, particularly concentrated over the EF-hand domain; however, a smaller patch of basic electrostatic potential exists over the SAM domain (Stathopulos et al. 2008).

The NMR structure reveals a basis for the compact nature of STIM1 EF-SAM. Internally within EF-SAM, the EF-hand pair forms a hydrophobic pocket in the Ca^{2+}-loaded state through the side chain orientation of at least 12 amino acids (i.e. Val68, Ile71, His72, Leu74, Met75, Val83, Leu92, Leu96, Lys104, Phe108, Ile115, Leu120) (Fig. 2.3B, left panel). This hydrophobic cleft serves as a dock for non-polar side chains protruding on the distal end of the α10 helix on the SAM domain (i.e. Leu195 and Leu199) (Fig. 2.3A, left panel) (Stathopulos et al. 2008). These intimate hydrophobic contacts between the EF-hand pair and the SAM domain lock STIM1 EF-SAM into a compact fold in the presence of Ca^{2+}, which auto-inhibits homotypic association of these domains and keeps STIM1 in a quiescent state. Disruption of the EF-hand:SAM domain interaction via mutation (i.e. Phe108Asp/Gly110Asp or Leu195Arg) facilitates oligomerization of STIM1 EF-SAM *in vitro*, and in live cells within the full-length STIM1 context independent of Ca^{2+} levels. *In vitro*, these EF-hand or SAM mutations cause the protein to adopt an apo-like structure, based on far-UV CD data, but do not alter the Ca^{2+} binding properties of EF-SAM. In live cells, these mutations result in a constitutive puncta formation of STIM1 and activation of SOCs even when the ER luminal Ca^{2+} stores are full (Stathopulos et al. 2008).

As expected from the high sequence conservation between STIM1 and STIM2 EF-SAM, the 3D NMR structure of Ca^{2+}-loaded STIM2 EF-SAM is homologous to STIM1 [i.e. backbone Cα, NH, CO root mean square deviation (rmsd) of 2.7 Å] (Fig. 2.3A, right panel) (Zheng et al. 2011). STIM2 EF-SAM also possesses a second, non-canonical EF-hand motif, suggesting that the EF-hand pair is an important structural feature of all STIMs. In conjunction with the canonical EF-hand, the non-ion-coordinating helix-loop-helix motif forms a hydrophobic pocket, more extensive than that observed for Ca^{2+}-loaded STIM1 EF-SAM. The STIM2 EF-hand non-polar cleft is created by 13 side chains with hydrophobic character (i.e. Leu72, Ile75, His76, Met79, Ile87, Phe95, Met100, Lys103, Lys108, Leu112, Ile119, Leu124, Trp128) (Fig. 2.3B, right panel). The Lys103 of STIM2 EF-SAM occurs as an aligned His (i.e. amino acid 99) in STIM1, and the Trp128 occurs as a conserved Trp124 in STIM1; moreover, His99 and Trp124 are directed away from the cleft in the STIM1 EF-SAM structure. The EF-hand domain Lys103 of STIM2 EF-SAM is oriented in close proximity with Asp200 on the α10 helix of the SAM domain, stabilizing the EF-hand:SAM domain interaction via charged interactions (Fig. 2.3A, right panel). The electrostatic surface potential of STIM2 EF-SAM is primarily acidic at neutral pH, with most surface acidic residues clustering in the EF-hand region of the protein (Zheng et al. 2011).

The SAM domain of STIM2 EF-SAM adopts the typical five-helix bundle topology characteristic of these protein-interaction domains (Qiao and Bowie 2005). Twelve

residues within the STIM2 SAM domain are greater than 95 % inaccessible to solvent (i.e. Leu142, Leu145, Val149, Phe158, Val163, Leu168, Met179, Ile180, Leu183, His190, Lys193, and Leu194) (Fig. 2.3C, right panel). In comparison, STIM1 buries 9 residues within the SAM domain core (Val137, Leu141, Val145, Leu159, Leu167, Met174, His186, Leu190, and Ala194) (Fig. 2.3C, left panel). The hydrophobic STIM2 Ile180 is not conserved in STIM1. This bulky Ile side chain facilitates a rearrangement of residues resulting in the insertion of Phe158 and Lys193 into the STIM2 SAM core (Zheng et al. 2011). These conserved Phe (i.e. amino acid 154) and Lys (i.e. amino acid 189) residues are excluded from the core in STIM1. The STIM2 SAM domain protrusion residues for interaction with the EF-hand pocket include the conserved Leu199 and Leu203 of α10 (Fig. 2.3A, right panel). The enlarged EF-hand hydrophobic cleft, the orientation of basic Lys103 on the EF-hand domain in close proximity to acidic Asp200 on the SAM domain, and the enhanced hydrophobic core of the SAM domain all contribute to the augmented stability and attenuated oligomerization propensity observed for STIM2 EF-SAM compared to STIM1.

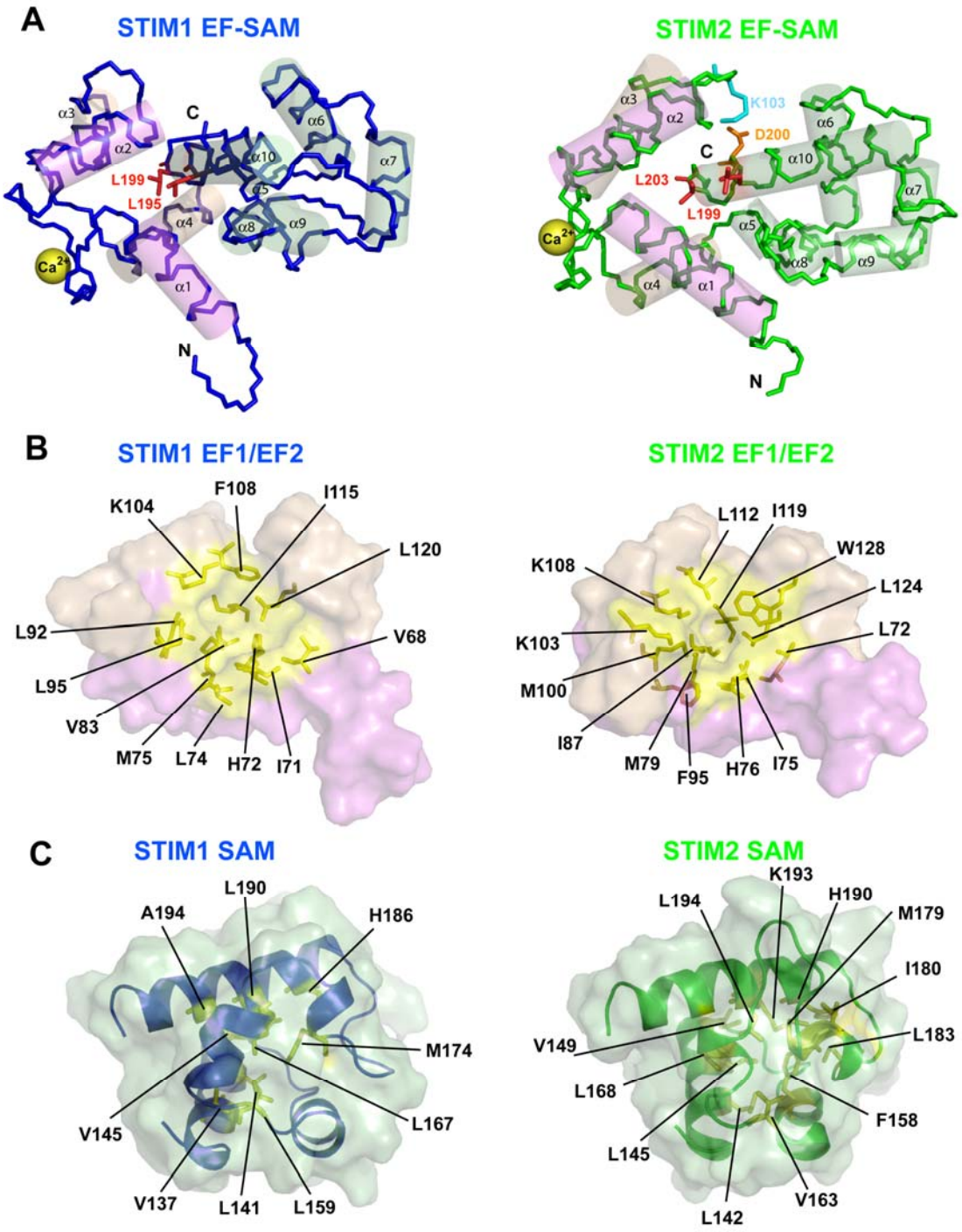

Fig. 2.3 *Atomic-resolution NMR structures of STIM1 and STIM2 EF-SAM. A. Structural features of holo EF-SAM proteins.* The backbone atoms of Ca^{2+}-loaded STIM1 and STIM2 EF-SAM are traced in blue (left structure) and green (right structure), respectively. The canonical EF-hand helices are shown in violet, the non-canonical EF-hand helices are in beige, and the linker and SAM helices are shown in green cylinders. The Ca^{2+} ions coordinated in the canonical loop are shown as yellow spheres and the carboxy (C) and amino (N)-termini are indicated. The critical α10 SAM anchor side chains are presented as red sticks. Unique to the STIM2 EF-SAM structure is the complementary positioning of the basic Lys103 (cyan sticks) and acidic Asp200 (orange sticks) side chains. *B. EF-hand cleft architecture of EF-SAM proteins*. A

surface representation of the EF-hand domains is shown for STIM1 (left) and STIM2 (right) where colouring is consistent with panel *A*. Residues (sticks) and associated surface forming the non-polar clefts are shown as yellow. ***C.*** *SAM domain hydrophobic core packing within EF-SAM proteins.* The STIM1 and STIM2 SAM backbones are shown as blue (left) and green (right) ribbon representations within the SAM domain surface, respectively. Side chains that are greater than 95% inaccessible to solvent are indicated with yellow sticks. STIM1 EF-SAM pdbID: 2K60.pdb; STIM2 EF-SAM pdbID: 2L5Y.pdb.

2.6 Extraneous Luminal Regions Involved in STIM Ca^{2+} Sensing

Considerable primary sequence variability exists within the luminal-oriented regions of STIM1 and STIM2 outside the EF-SAM domains (Fig. 2.1B). These extraneous residues influence Ca^{2+} sensing and regulation of CRAC entry by STIMs. The extension of STIM1 EF-SAM to include all luminal residues outside the signal peptide (i.e. amino acids 23 – 213) enhances the stability in the presence and absence of Ca^{2+} (Stathopulos et al. 2009). A STIM2 construct engineered with similar aligned boundaries is susceptible to C-terminal degradation; however, a somewhat shorter, degradation-resistant STIM2 protein (i.e. amino acids 15 – 205) also shows an enhanced stability compared to EF-SAM *in vitro*. Far-UV CD data of these extended EF-SAM constructs show less α-helicity per residue in the presence of Ca^{2+} compared to the minimal EF-SAMs, suggesting that the extraneous residues may have a more prominent effect on the unfolded states of EF-SAM (Stathopulos et al. 2009). In live cells, swapping STIM1 residues 1 – 65 (i.e. including the STIM1 signal peptide) with STIM2 residues 1 – 69 and *vice versa* exchanges the CRAC activation phenotype, where full-length STIM1 harboring the STIM2 N-terminal residues exhibits a delay in Orai1 activation and STIM2 fused to the STIM1 N-terminal residues demonstrates wild-type STIM1 CRAC activation kinetics (Zhou et al. 2009).

Two conserved cysteine residues (i.e. Cys49 and Cys56 in STIM1) are encoded in the N-terminal residues extraneous to EF-SAM. Oxidant-induced *S*-glutathionylation of Cys56 in STIM1 results in constitutive puncta and CRAC entry, suggesting that this Cys residue may afford STIM1 with an additional Ca^{2+}-independent, oxidant-dependent sensory function (Hawkins et al. 2010).

The open reading frame of STIM2 extends 87 residues upstream of the previously determined non-AUG translational start site (Fig: 1B) (Williams et al. 2001). Recent data suggests that these 87 upstream residues in addition to the predicted STIM2 ER signal peptide downstream of the non-AUG start site (i.e. residues 88 – 101; numbering 1 – 14 downstream of the non-AUG start site) are required for STIM2 to insert into the ER membrane (Graham et al. 2011). With this exceedingly long 101 residue signal peptide, a fraction of STIM2 remains cytosolic, activating PM Orai1 CRAC channels associated with basal Ca^{2+} homeostasis. Interestingly, the 101 amino acid signal peptide that is cleaved from the ER-inserted STIM2 pre-protein may have a function in Ca^{2+}- and SOCE-independent regulation of gene transcription (Graham et al. 2011).

2.7 STIM1 TM Structure

Recently, it has been shown that the STIM1 TM region is homodimerized in the resting state, and changes in the nature of the TM:TM interaction can modulate the position of the adjacent CC1 regions within STIM1 dimers (Ma et al. 2015). Specifically, solution NMR experiments of the STIM1 TM region (i.e. residues 209-237) reconstituted in

bicelles show chemical shift perturbations for Gly225, Gly226, Trp228, Gln233 and Asn234 after incorporation of a constitutively active Cys227Trp mutation. Further, chemical crosslinking and fluorescence resonance energy transfer (FRET) experiments demonstrated that the N-terminal residues of the STIM1 TM region come into close proximity of one another in this mutation-mediated activated state while closely apposing the N-terminal region of the CC1 domains, consistent with EF-SAM induced dimerization/oligomerization of the region (Ma et al. 2015).

2.8 STIM1 CC1 Structure

STIMs contain three conserved CC regions immediately after the TM domain (i.e. CC1, CC2 and CC3). By crystallography, the STIM1 Met244Leu/Leu321Met CC1 double mutant encompassing residues 237-340 adopts an elongated α-helical structure that extends from the N-terminus to the C-terminus and spans ~13 nm (Cui et al. 2013). This extended conformation would bridge the bulk of the necessary distance between the ER and PM for direct STIM1 coupling to Orai1 channels and STIM1 interaction with PM phosphoinositides (Calloway et al. 2011; Korzeniowski et al. 2009; Liou et al. 2007; Walsh et al. 2010), although this construct does not contain the necessary machinery for these heteromeric protein or lipid interactions. The CC1 molecules dimerize in the crystalline state in an antiparallel manner with the C-termini clustered close together; moreover, deletion of the C-terminal region of this construct (i.e. Δ311-340) results in persistent monomerization in solution. Within the crystal, hydrophobic interactions between Leu335, Leu328, Val324 and Ala317 of one subunit and Leu286, Ile290, Ala293 and Leu300 of the partner subunit, H-bonding between Leu303, Arg304 and Thr307 of one subunit and Glu310 and Gln314 of the partner subunit and an ionic bond involving Arg304 and Glu318 on opposite subunits are the main forces mediating dimerization through the C-terminal ends (Fig. 2.4A). The dimerization interface and proximity of the C-terminal ends (i.e. residues 310-340) observed in the CC1 double mutant crystal structure is inconsistent with the orientation of the same region in the *Caenorhabditis elegans* SOAR crystal structure (Yang et al. 2012) (see Chap. 2.9) where the structures overlap, implying that this helix within STIM1 is capable of undergoing extensive conformational dynamics.

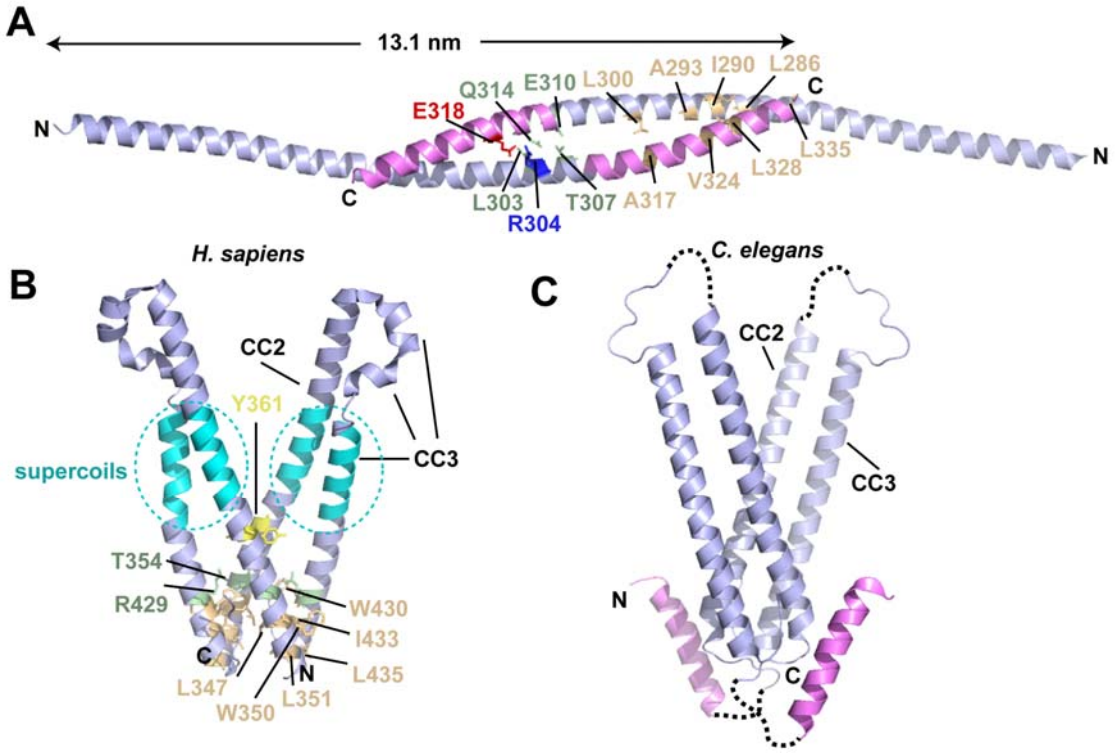

Fig. 2.4 *Atomic-resolution crystal structures of STIM CC domains. A. Structural features of the extended human CC1 domain.* Residues participating in intermolecular hydrophobic interactions (light orange), H-bonding (light green) and ionic bonds (acidic – red; basic – blue) are presented as sticks. The portion of the CC1 helix previously demonstrated to play a role in modulating the activity of STIM1 is indicated (light magenta). *B. Structural features of the human Leu374Met/Val419Ala/Cys436Thr SOAR/CAD/ccb9 domain.* The V-shape dimer is shown with the regions between CC2 and CC3 that undergo supercoiling coloured cyan. The intermolecular forces stabilizing the dimer are indicated with residues involved in hydrophobic interactions (light orange), H-bonding (light green) and aromatic side chain stacking (yellow) drawn as sticks. *C. Structural features of the C. elegans CC1-CAD region.* The homologous CC1 region previously revealed to play a role in modulating the activity of human STIM1 is coloured light magenta (i.e. similar to the region shown in *A.*). In *A. – C.*, the amino and carboxy termini are indicated by N and C, respectively.

2.9 STIM1 CC2-CC3 (SOAR/CAD/ccb9) Structure

The crystal structure of the human STIM1 SOAR/CAD/ccb9 region (i.e. residues 345-444) has been solved at ~1.9 Å (Yang et al. 2012) using a Leu374Met/Val419Ala/Cys436Thr triple mutant protein with inhibited propensity for aggregation and stabilized dimeric structure. This symmetric dimer buries ~1800 $Å^2$, with the two monomers arranged in a V-shape (Fig. 2.4B). Each monomer in the human protein contains an extended CC2 helix, followed by two short and one extended α-helix, which makes up the CC3 region and is antiparallel to CC2. Although the V-shaped dimer architecture is structurally conserved, the three broken helices making up the CC3 region are distinct in the human homologue compared to the *C. elegans* structure which shows a continuous CC3 region (Fig. 2.4C). No intermolecular supercoiling exists between the CC regions; however, intramolecular supercoiling can be identified between the CC2 (i.e. residues Lys366 to Ala376) and CC3 (i.e. residues Ile409 to Ala419) regions of each

monomer. Critical residues stabilizing the dimer interface include Leu347, Trp350, and Leu351 from one monomer hydrophobically interacting with Leu436, Ile433, and Trp430 of the partner subunit. Further, Thr354 forms an H-bond with Arg429 of the partner subunit, and Tyr361 homotypically stacks between subunits.

The structure of a *C. elegans* construct that is extended relative to the aforementioned human protein reveals an additional α-helix in the CC1 region, packing against CC2 and CC3 in an intramolecular and intermolecular manner, respectively (Fig. 2.4C). Deletion of the equivalent CC1 region in human STIM1 (i.e. Δ310-337 human residues) endows STIM1 with the ability to constitutively activate CRAC channels when co-overexpressed with Orai1 in live cells. However, different mutations in this CC1 helix, as opposed to full deletion, can constitutively activate as well as inhibit CRAC entry (Stathopulos et al. 2013; Yu et al. 2013). Thus, this region of CC1 plays an important modulatory role in the conformational change that occurs in the cytosolic domains, requisite for the recruitment and activation of Orai CRAC channels at ER-PM junctions.

2.10 *D. melanogaster* Orai Structure

A crystal structure of the *D. melanogaster* Orai homologue encompassing residues 132-341 (i.e. an N- and C-terminally truncated form of *D. melanogaster*) and carrying a Cys224Ser/Cys283Thr/Pro276Arg/Pro277Arg quadruple mutation to produce well-diffracting crystals (i.e. ~3.4 Å) has been elucidated (Hou et al. 2012). The TM regions of the *D. melanogaster* homologue are > 70 % identical with the human Orai1 form of the protein. Remarkably, this Orai crystal structure exhibits a six-fold central axis of symmetry along the pore and overall three-fold symmetry due to differences in the TM4 orientation within the dimer building blocks of the hexamer (Fig. 2.5A). The hexameric quaternary state is in contrast to several studies suggesting that Orai1 assembles as a functional tetramer (Demuro et al. 2013; Maruyama et al. 2009; Mignen et al. 2008; Penna et al. 2008; Thompson and Shuttleworth 2013). TM1 helices line the pore in the oligomeric structure, and a circle composed of Glu178 corresponding to human Glu106 near the extracellular surface of the assembled channel is vital for Ca^{2+} binding and ion permeability (Fig. 2.5B). Central in the pore is a hydrophobic core made up of Leu167, Phe171 and Val174 that correspond to human Orai1 Leu95, Phe99, Val102 (Fig. 2.5B). Finally, on the intracellular side, the pore surface of TM1 is lined by Arg155, Lys159 and Lys163, corresponding to Arg83, Lys87 and Arg91 in human Orai1 (Fig. 2.5B). The Lys163Trp mutation (i.e. Arg91Trp mutation in humans) associated with a heritable form of severe combined immunodeficiency disease (SCID) introduces a bulky hydrophobic residue that points into the center axis of the pore. Thus, channel dysfunction associated with SCID may be due to an inability of the pore to dilate and allow the Ca^{2+} ion to move from the anionic entrance through the hydrophobic core and beyond the cationic base on the intracellular side of the pore.

Each TM1 helix extends in a linear manner beyond the inner face of the PM into the cytosol. On the other hand, the C-terminal domains, which are extensions of the TM4 helices, run primarily parallel to the inner plane of the PM due to the presence of a hinge (*i.e.* residues 305-308) region that bends the extensions in two possible conformations (Fig. 2.5C). The two conformations arrange the C-terminal helices in an antiparallel manner such that they are stabilized by inter-subunit hydrophobic interactions between Ile316 and Leu319 of the opposite subunit (i.e. Phe270 and Leu273 in human

numbering). Considering that deletion of the C-terminal cytosolic extension disrupts interactions with STIM1 (McNally et al. 2013; Park et al. 2009; Zheng et al. 2013), the supercoiled helix pair may represent a vital structural architecture that permits interactions with Ca^{2+}-depleted and oligomerized STIM1 at ER-PM junctions, consistent with solution NMR work revealing a structural complex between the Orai1 C-terminal helices and the STIM1 CC domains (see Chap. 2.11) (Stathopulos et al. 2013).

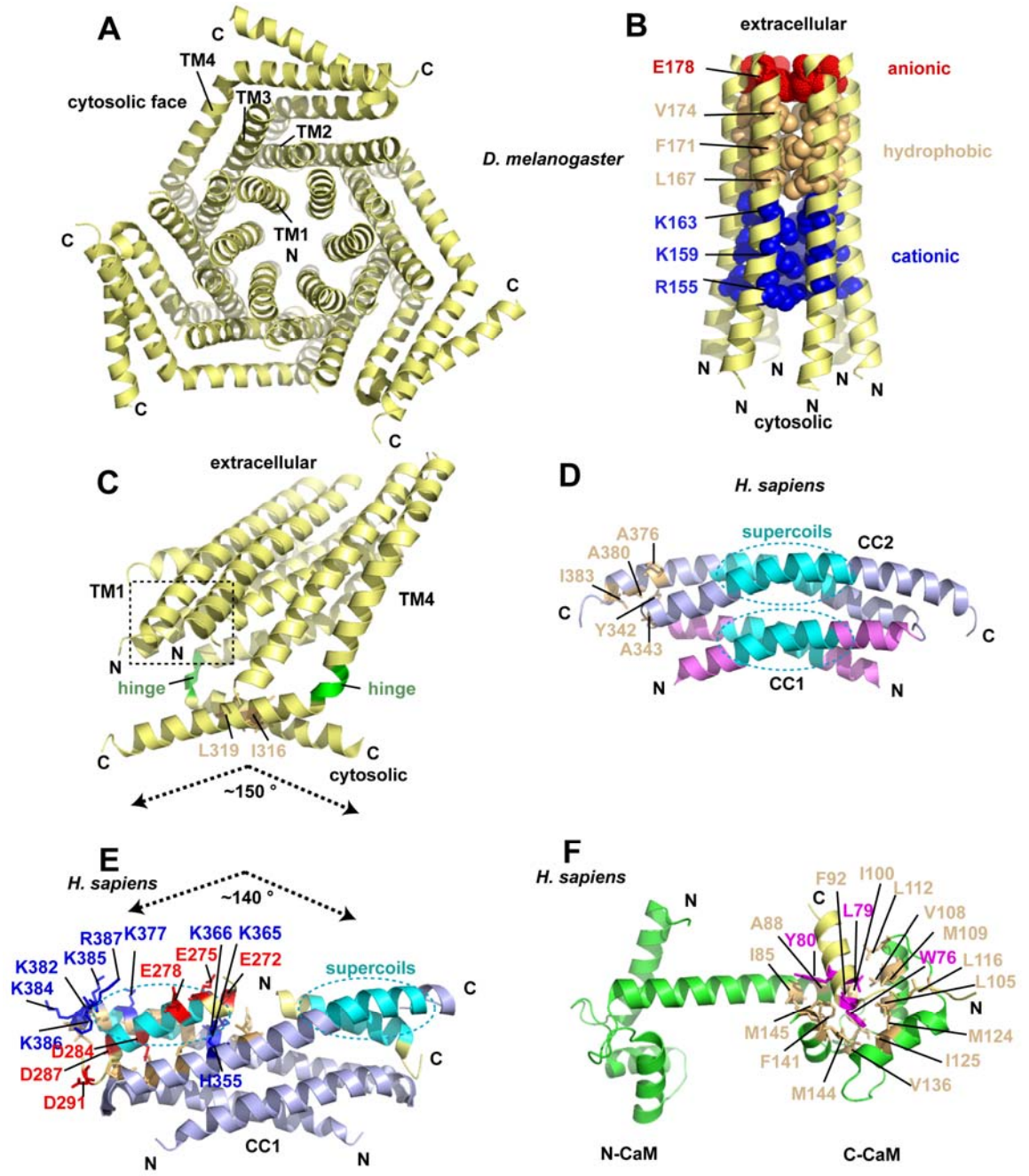

Fig. 2.5 *Atomic resolution structures of Orai alone as well as in complex with the STIM1 CC region and CaM. A. Hexamer architecture of truncated Cys224Ser/Cys283Thr/Pro276Arg/Pro277Arg D. melanogaster Orai revealed by the crystal structure.* The relative positions of TM1-TM4 within one monomer are indicated. The TM1 helices exhibit a six-fold pore symmetry while the two possible C-

terminal domain conformations result in an outer three-fold symmetry. *B. Anionic-hydrophobic-cationic pore architecture of D. melanogaster Orai.* Residues conferring anionic (red), hydrophobic (light orange) and cationic (blue) properties are indicated by spheres. *C. Multiple C-terminal domain conformations and TM1 extensions in the dimer units of D. melanogaster Orai.* The hinge regions (green) in the TM4 extensions facilitating the antiparallel orientation of the C-terminal domains and the residues involved in stabilizing hydrophobic interactions of this region (light orange sticks) are shown. The interhelical angle of the C-terminal domain is highlighted by the dashed arrows. The TM1 N-terminal extension is indicated by a dashed box. *D. Orai1-free solution conformation of the wild-type human STIM1 CC1-CC2 region.* The residues undergoing supercoiling in the CC1 and CC2 region are coloured cyan. The CC1 region previously demonstrated to modulate the activity of STIM1 is coloured magenta (i.e. analogous to Fig. 4A and 4C). Hydrophobic residues mediating intermolecular CC2:L1 interactions that stabilize the Orai1-free conformation are shown as light orange sticks. *E. Orai1 C-terminal domain-bound solution conformation of the wild-type human STIM1 CC1-CC2 region.* The hydrophobic (light orange) and basic residues (blue) making up the SOAP are shown as sticks. Hydrophobic residues making up the SOAP are not labeled for simplicity. The Orai1 C-terminal domain peptides (i.e. residues 272-292) are coloured yellow and the intermolecular regions of supercoiling are cyan. The acidic residues on the Orai1 C-terminal domain peptides that interact with the basic rim are shown as red sticks. Only one of the two interacting Orai1 C-terminal peptides is annotated for simplicity. The interhelical angle of the human Orai1 C-terminal peptides is highlighted by the dashed arrows. *F. Crystal structure of the human Orai1 N-terminal domain extension bound to CaM.* The dumbbell structure of CaM is shown in green. The residues forming the hydrophobic pocket (light orange) on the C-terminal domain of CaM (C-CaM) are indicated. The Orai1 N-terminal domain extension (i.e. residues 68-91) is coloured yellow. The Orai1 N-terminal residues that anchor into the C-CaM cleft are illustrated in magenta. In *A.* – *F.*, the amino and carboxy termini are labeled N and C, respectively.

2.11 STIM1 CC1[TM-distal]-CC2 Structure and Complexation with the Orai1 C-terminal Domain

The human STIM1 $CC1_{[TM\text{-}distal]}$-CC2 fragment consisting of residues 312-387 is composed of two α-helices (i.e. α1, residues 313-340; α2, residues 344-382) connected by a short linker loop (i.e. L1, residues 341-343). Based on structural evidence from solution NMR spectroscopy, these U-shaped monomeric fragments form symmetric antiparallel dimers via α1:α1' (i.e. CC1:CC1), α2:α2' (i.e. CC2:CC2) and C-terminal α2:L1' (i.e. CC2:L1) interactions. Specifically, residues 320-331 of each monomer form the antiparallel CC1 supercoil, residues 355-369 form the antiparallel CC2 supercoil and residues Ala376, Ala380 and Ile383 of C-terminal α2/CC2 interact with residues Tyr342' and Ala343' of L1' (Fig. 2.5D).

Solution NMR spectroscopy also showed that this region of STIM1 can interact with an Orai1 C-terminal fragment consisting of residues 272-292. NMR titration revealed that residues Glu272, Leu273, Asn274, Ala277, Glu278, Ala280, Arg281, His288 and Arg289 of Orai1 $C_{272\text{-}292}$ undergo the most pronounced chemical shift perturbations upon binding to STIM1 $CC1_{[TM\text{-}distal]}$-CC2. Within dimeric STIM1 $CC1_{[TM\text{-}distal]}$-CC2, residues Pro344, Leu347, Leu351, His355 and Val359 of N-terminal α2 and residues Tyr362', Lys366', Ala369', Leu373', Ala376', Ala380' and Ile383' of C-terminal α2' all contribute to the binding of Orai1 $C_{272\text{-}292}$. Specifically, Orai1 Asn274, Ala277, Arg281, Gln285 and Arg289 residues interact with STIM1 N-terminal α2 whereas Orai1 Leu273, Leu276, Ala280, Gln283 and Leu286 residues interact with STIM1 C-terminal α2'. This STIM-Orai association pocket (SOAP) that has extensive hydrophobicity in the central cavity is also surrounded by a basic rim of residues for electrostatic interactions (Fig. 2.5E). His355, Lys365', Lys366', Lys377', Lys382', Lys384', Lys385', Lys386' and Arg387'

of the α2 helix form the basic rim which complement the Glu272, Glu275, Glu278, Asp284, Asp287 and Asp291 acidic residues on the Orai1 $C_{272-292}$ surface.

The importance of each of the α1: α1', α2: α2' and α2:L1' interfaces elucidated by the solution NMR structures in the activation of CRAC entry have been assessed. Interestingly, the Glu318Gln/Glu319Gln/Glu320Gln/Glu322Gln (4EQ) charge-neutralizing quadruple mutation stabilizes STIM1 α1:α1' interface, enhances dimerization, increases its interaction with Orai1 $C_{272-292}$ and promotes spontaneous inward-rectifying currents; in contrast, the Val324Pro α1 helix-breaking mutation destabilizes the STIM1 α1:α1' interface, attenuates dimerization, decreases its interaction with Orai1 $C_{272-292}$ and lowers the maximal inward currents. The STIM1 α2 Tyr361Lys/Tyr362Lys double mutant cannot activate CRAC channels due to destabilization of the $CC1_{[TM\text{-}distal]}$-CC2 dimer and abrogation of binding to Orai1 $C_{272-292}$. Therefore, the α1:α1' interface plays a role in the efficiency and α2:α2' interface is essential for CRAC channel activation. The Lys382Glu/Lys384Glu/Lys385Glu/Lys386Glu (4KE) quadruple mutation on the basic C-terminal α2 helix does not significantly affect the stability or dimerization of STIM1 $CC1_{[TM\text{-}distal]}$-CC2; however, this 4KE mutation prevents interactions with Orai1 $C_{272-292}$, indicating that the α2:L1' interface only marginally affects STIM1 $CC1_{[TM\text{-}distal]}$-CC2 dimerization, but the C-terminal α2 residues play an important role in Orai1-mediated activation of CRAC channels.

Interestingly, there are striking similarities between the *D. melanogaster* Orai crystal structure and the solution structure for *H. sapiens* Orai1 $C_{272-292}$ in complex with STIM1 $CC1_{[TM\text{-}distal]}$-CC2. First, the *D. melanogaster* Orai C-terminal helices are in antiparallel conformation, as is observed with the human Orai1 $C_{272-292}$ peptides. Second, the interhelical angle between the *D. melanogaster* Orai cytosolic C-terminal helices is 152°, analogous to the obtuse angle of 136° revealed in the *H. sapiens* complex structure (Fig. 2.5C and 2.5E). Finally, docking of three $CC1_{[TM\text{-}distal]}$-CC2: Orai1 $C_{272-292}$ dimers onto the *D. melanogaster* Orai hexamer by structural alignment of the homologous residues of the C-termini illustrates a steric compatibility at the assembled hexameric level (Stathopulos et al. 2013). Remarkably, the putative CC3 locations after the docking are adjacent to one another and poised for CC3:CC3' interactions that enhance oligomerization, as previously observed for this region of STIM1 experimentally (Covington et al. 2010; Muik et al. 2009). Consistent with this mode of STIM1:Orai1 $C_{272-292}$ interaction, it has been shown that disruption of the bend architecture preceding the cytosolic C-termini facilitates the antiparallel Orai1 C-terminal domain arrangement that abolishes binding, and locking of the Orai1 C-terminal bend with the incorporation of a Cys-mediated disulfide still permits binding to STIM1 CC2-CC3 (Tirado-Lee et al. 2015). Additionally, C-terminal deletion mutants found to abrogate binding to STIM1, among several variable length deletions of the Orai1 C-terminal domain, are consistent with the interaction mode revealed by the solution NMR structure (Palty et al. 2015).

2.12. CaM Structure and Complexation with the Orai1N-terminal Domain

CRAC channels undergo a Ca^{2+}-dependent inactivation (CDI) phenomenon via the actions of STIM1 and CaM (Derler et al. 2009; Mullins et al. 2009; Roos et al. 2005). Residues located C-terminal to the CC3 region of STIM1 (i.e. residues 470-491) have been linked to the fast CDI of CRAC channels (Mullins et al. 2009). Further, Ca^{2+}-loaded

CaM has been demonstrated to bind to the polybasic tails of both STIM1 (i.e. residues 667-685) and STIM2 (i.e. residues 730-746) with μM affinity (Bauer et al. 2008). Therefore, CaM may downregulate SOCE activity by inhibiting and/or disrupting ER-PM relocalization of STIM molecules that occurs via interactions of the polybasic STIM C-termini with phosphoinositides (Calloway et al. 2011; Korzeniowski et al. 2009; Liou et al. 2007; Walsh et al. 2010; Yuan et al. 2009). Ca^{2+}-loaded CaM also binds to the Orai1 N-terminal domain (i.e. residues 68-91), and interaction of CaM with this Orai1 N-terminal region has been implicated in the CDI of CRAC channels (Mullins et al. 2009). A complex structure of a human Orai1 N-terminal fragment encompassing residues 69-91 interacting with CaM has been solved at 1.9 Å. This crystal structure shows Ca^{2+}-loaded CaM adopts the well-characterized dumbbell structure where each lobe is separated by an extended α-helical linker; however, only the C-terminal lobe shows the presence of the Orai1-N peptide (Fig. 2.5F). The interaction observed in this crystal complex occurs primarily via Trp76, Leu79 and Tyr80 hydrophobic side chains packing into the CaM C-terminal domain cleft made up of Ile85, Ala88, Phe92, Ile100, Leu105, Val108, Met109, Leu112, Leu116, Met124, Ile125, Val136, Phe141, Met144 and Met145 (Fig. 2.5F).

Although the crystal structure does not reveal the mode of binding of the Orai1-N peptide to the CaM N-terminal domain, solution experiments indeed show that an interaction occurs with lower affinity on this CaM domain (Derler et al. 2013). Since the Orai1 N-terminal domain binds independently to both the CaM N- and C-terminal domains, it is possible that the CDI mechanism involves bridging two Orai1 N-termini within the Orai1 tetramer or hexamer complex (Liu et al. 2012).

2.13 Concluding Remarks

Four fundamental features contribute to the Ca^{2+} sensing function of EF-SAM domains: (*i*) the binding affinity of the canonical EF-hand, (*ii*) the nature of the EF-hand hydrophobic cleft mutually formed by the canonical and non-canonical EF-hand motifs, (*iii*) the stability of the EF-hand:SAM domain interaction, and (*iv*) the local stability of the SAM domain core. These four elements are not mutually exclusive, but are inter-dependent during Ca^{2+} sensing. Upon Ca^{2+} dissociation from the canonical EF-hand loop, the EF-hand:SAM domain interaction which auto-inhibits oligomerization of this domain is destabilized, resulting in a coupled oligomerization. This oligomerization instigates a TM region rearrangement, which closely apposes the N-terminal CC1 domains within STIM dimers and triggers a cytosolic CC reorganization that promotes interactions with the PM lipids at ER-PM junctions. Punctate STIM molecules directly couple to Orai1 C- and N-terminal domains in the recruitment of Orai1 and gating of assembled CRAC channels. Differences in the CAD/SOAR/ccb9 (i.e. CC2-CC3), CC1-CAD/SOAR/ccb9 (Yang et al. 2012), CC1 (Cui et al. 2013) crystal structures and solution NMR data on CC1-CC2 fragments solved in the absence and presence of Orai (Stathopulos et al. 2013), are in line with the dynamic closed-to-open transition that the STIM1 cytosolic domains must undergo to adopt an Orai recruitment- and activation-competent conformation (Fahrner et al. 2014; Korzeniowski et al. 2011; Korzeniowski et al. 2016; Maus et al. 2015; Muik et al. 2011; Yu et al. 2013; Zhou et al. 2013). The antiparallel C-terminal domain extensions of TM4 (Hou et al. 2012) present Orai C-terminal binding sites to STIM molecules at ER-PM junctions during the activation process. Further, the Orai1 C-terminal antiparallel domain orientation of the *D. melanogaster* Orai structure is

remarkably consistent with the geometry of assembly observed in the human STIM1 CC1-CC2:Orai1 $C_{272-292}$ complex structure (Stathopulos et al. 2013), providing a compelling coupling mechanism between the two principle players of SOCE.

Despite the tremendous progress in elucidating atomic details of the features involved in regulating CRAC channels and SOCE, several important structural questions remain unanswered. The precise structure of the Ca^{2+}-depleted EF-SAM domain is unknown; further the manner in which the wild-type human CAD/SOAR/ccb9 region interacts with human Orai1-constituted channels remains unknown. Additionally, the open conformation of the full-length native Orai1 channel has not been resolved; similarly, the closed native human Orai1 channel structure has not been elucidated. The structural basis for STIM homomeric intermolecular CC3 interactions involved in oligomerization and potential interactions with the Orai proteins during the activation process is also unknown. The basis for Orai1 N-terminal binding to STIM1, which has been implicated in channel recruitment and gating, has not been disseminated. Additionally, the precise stoichiometry of the functional STIM:Orai complex requires further clarification.

Acknowledgements

This work was supported by a Natural Sciences and Engineering Research Council of Canada Discovery Grant to P.B.S. and Canadian Institutes of Health Research Operating Grant to Q.F., P.B.S. and W.Y.L.. We thank Mitsuhiko Ikura for his invaluable contributions in preparing the first edition version of this chapter.

References

Baba Y, Hayashi K, Fujii Y, Mizushima A, Watarai H, Wakamori M, Numaga T, Mori Y, Iino M, Hikida M, Kurosaki T (2006) Coupling of STIM1 to store-operated Ca2+ entry through its constitutive and inducible movement in the endoplasmic reticulum. Proc Natl Acad Sci U S A 103:16704–16709

Balasuriya D, Srivats S, Murrell-Lagnado RD, Edwardson JM (2014) Atomic force microscopy (AFM) imaging suggests that stromal interaction molecule 1 (STIM1) binds to Orai1 with sixfold symmetry. FEBS Lett 588:2874–2880

Bauer MC, O'Connell D, Cahill DJ, Linse S (2008) Calmodulin binding to the polybasic C-termini of STIM proteins involved in store-operated calcium entry. Biochemistry 47:6089–6091

Berna-Erro A, Braun A, Kraft R, Kleinschnitz C, Schuhmann MK, Stegner D, Wultsch T, Eilers J, Meuth SG, Stoll G, Nieswandt B (2009) STIM2 regulates capacitive Ca2+ entry in neurons and plays a key role in hypoxic neuronal cell death. Sci Signal 2:ra67

Berridge MJ, Lipp P, Bootman MD (2000) The versatility and universality of calcium signalling. Nat Rev Mol Cell Biol 1:11–21

Berridge MJ, Bootman MD, Roderick HL (2003) Calcium signalling: dynamics, homeostasis and remodelling. Nat Rev Mol Cell Biol 4:517–529

Berridge MJ (2009) Cell Signaling Biology. http://www.cellsignallingbiology.org

Bird GS, Hwang SY, Smyth JT, Fukushima M, Boyles RR, Putney JW Jr. (2009) STIM1 is a calcium sensor specialized for digital signaling. Curr Biol 19:1724–1729

Bootman MD, Lipp P (2001) Calcium signalling and regulation of cell function. Encyclopedia of Life Sciences 1–7

Brandman O, Liou J, Park WS, Meyer T (2007) STIM2 is a feedback regulator that stabilizes basal cytosolic and endoplasmic reticulum Ca2+ levels. Cell 131:1327–1339

Cai X (2007) Molecular evolution and structural analysis of the Ca(2+) release-activated Ca(2+) channel subunit, Orai. J Mol Biol 368:1284–1291

Calloway N, Owens T, Corwith K, Rodgers W, Holowka D, Baird B (2011) Stimulated association of STIM1 and Orai1 is regulated by the balance of PtdIns(4,5)P(2) between distinct membrane pools. J Cell Sci 124:2602–2610

Collins SR, Meyer T (2011) Evolutionary origins of STIM1 and STIM2 within ancient Ca(2+) signaling systems. Trends Cell Biol 21:202–211

Covington ED, Wu MM, Lewis RS (2010) Essential role for the CRAC activation domain in store-dependent oligomerization of STIM1. Mol Biol Cell 21:1897–1907

Cui B, Yang X, Li S, Lin Z, Wang Z, Dong C, Shen Y (2013) The inhibitory helix controls the intramolecular conformational switching of the C-terminus of STIM1. PLoS One 8:e74735

Demuro A, Penna A, Safrina O, Yeromin AV, Amcheslavsky A, Cahalan MD, Parker I (2013) Subunit stoichiometry of human Orai1 and Orai3 channels in closed and open states. Proc Natl Acad Sci U S A 108:17832–17837

Derler I, Fahrner M, Muik M, Lackner B, Schindl R, Groschner K, Romanin C (2009) A CRAC modulatory domain (CMD) within STIM1 mediates fast Ca2+-dependent inactivation of ORAI1 channels. J Biol Chem 284:24933–24938

Derler I, Plenk P, Fahrner M, Muik M, Jardin I, Schindl R, Gruber HJ, Groschner K, Romanin C (2013) The extended transmembrane Orai1 N-terminal (ETON) region combines binding interface and gate for Orai1 activation by STIM1. J Biol Chem 288:29025–29034

Fahrner M, Muik M, Schindl R, Butorac C, Stathopulos P, Zheng L, Jardin I, Ikura M, Romanin C (2014) A coiled-coil clamp controls both conformation and clustering of stromal interaction molecule 1 (STIM1). J Biol Chem 289:33231–33244

Feske S, Gwack Y, Prakriya M, Srikanth S, Puppel SH, Tanasa B, Hogan PG, Lewis RS, Daly M, Rao A (2006) A mutation in Orai1 causes immune deficiency by abrogating CRAC channel function. Nature 441: 179–185

Feske S (2007) Calcium signalling in lymphocyte activation and disease. Nat Rev Immunol 7:690–702

Frischauf I, Muik M, Derler I, Bergsmann J, Fahrner M, Schindl R, Groschner K, Romanin C (2009) Molecular Determinants of the Coupling between STIM1 and Orai Channels: DIFFERENTIAL ACTIVATION OF Orai1-3 CHANNELS BY A STIM1 COILED-COIL MUTANT. J Biol Chem 284:21696–21706

Graham SJ, Dziadek MA, Johnstone LS (2011) A cytosolic STIM2 preprotein created by signal peptide inefficiency activates ORAI1 in a store-independent manner. J Biol Chem 286:16174–16185

Hawkins BJ, Irrinki KM, Mallilankaraman K, Lien YC, Wang Y, Bhanumathy CD, Subbiah R, Ritchie MF, Soboloff J, Baba Y, Kurosaki T, Joseph SK, Gill DL, Madesh M (2010) S-glutathionylation activates STIM1 and alters mitochondrial homeostasis. J Cell Biol 190:391–405

Hou X, Pedi L, Diver MM, Long SB (2012) Crystal structure of the calcium release-activated calcium channel Orai. Science 338:1308–1313

Huang GN, Zeng W, Kim JY, Yuan JP, Han L, Muallem S, Worley PF (2006) STIM1 carboxyl-terminus activates native SOC, I(crac) and TRPC1 channels. Nat Cell Biol 8:1003–1010

Huang Y, Zhou Y, Wong HC, Chen Y, Wang S, Castiblanco A, Liu A, Yang JJ (2009) A single EF-hand isolated from STIM1 forms dimer in the absence and presence of Ca2+. Febs J 276:5589–5597

Korzeniowski MK, Popovic MA, Szentpetery Z, Varnai P, Stojilkovic SS, Balla T (2009) Dependence of STIM1/Orai1-mediated calcium entry on plasma membrane phosphoinositides. J Biol Chem 284:21027–21035

Korzeniowski MK, Manjarres IM, Varnai P, Balla T (2011) Activation of STIM1-Orai1 involves an intramolecular switching mechanism. Sci Signal 3:ra82

Korzeniowski MK, Baird B, Holowka D (2016) STIM1 activation is regulated by a 14 amino acid sequence adjacent to the CRAC activation domain. AIMS Biophys 3:99–118

Larkin MA, Blackshields G, Brown NP, Chenna R, McGettigan PA, McWilliam H, Valentin F, Wallace IM, Wilm A, Lopez R, Thompson JD, Gibson TJ, Higgins DG (2007) Clustal W and Clustal X version 2.0. Bioinformatics 23:2947–2948

Li Z, Lu J, Xu P, Xie X, Chen L, Xu T (2007) Mapping the interacting domains of STIM1 and Orai1 in Ca2+ release-activated Ca2+ channel activation. J Biol Chem 282:29448–29456

Liou J, Kim ML, Heo WD, Jones JT, Myers JW, Ferrell JE Jr., Meyer T (2005) STIM is a Ca2+ sensor essential for Ca2+-store-depletion-triggered Ca2+ influx. Curr Biol 15:1235–1241

Liou J, Fivaz M, Inoue T, Meyer T (2007) Live-cell imaging reveals sequential oligomerization and local plasma membrane targeting of stromal interaction molecule 1 after Ca2+ store depletion. Proc Natl Acad Sci U S A 104:9301–9306

Liu Y, Zheng X, Mueller GA, Sobhany M, DeRose EF, Zhang Y, London RE, Birnbaumer L (2012) Crystal structure of calmodulin binding domain of orai1 in complex with Ca2+ calmodulin displays a unique binding mode. J Biol Chem 287:43030–43041

Luik RM, Wu MM, Buchanan J, Lewis RS (2006) The elementary unit of store-operated Ca2+ entry: local activation of CRAC channels by STIM1 at ER-plasma membrane junctions. J Cell Biol 174:815–825

Luik RM, Wang B, Prakriya M, Wu MM, Lewis RS (2008) Oligomerization of STIM1 couples ER calcium depletion to CRAC channel activation. Nature 454:538–542

Ma G, Wei M, He L, Liu C, Wu B, Zhang SL, Jing J, Liang X, Senes A, Tan P, Li S, Sun A, Bi Y, Zhong L, Si H, Shen Y, Li M, Lee MS, Zhou W, Wang J, Wang Y, Zhou Y (2015) Inside-out Ca(2+) signalling prompted by STIM1 conformational switch. Nat Commun 6:7826

Manji SS, Parker NJ, Williams RT, van Stekelenburg L, Pearson RB, Dziadek M, Smith PJ (2000) STIM1: a novel phosphoprotein located at the cell surface. Biochim Biophys Acta 1481:147–155

Maruyama Y, Ogura T, Mio K, Kato K, Kaneko T, Kiyonaka S, Mori Y, Sato C (2009) Tetrameric Orai1 is a teardrop-shaped molecule with a long, tapered cytoplasmic domain. J Biol Chem 284:13676–13685

Maus M, Jairaman A, Stathopulos PB, Muik M, Fahrner M, Weidinger C, Benson M, Fuchs S, Ehl S, Romanin C, Ikura M, Prakriya M, Feske S (2015) Missense mutation in immunodeficient patients shows the multifunctional roles of coiled-coil domain 3 (CC3) in STIM1 activation. Proc Natl Acad Sci U S A 112:6206–6211

McNally BA, Yamashita M, Engh A, Prakriya M (2009) Structural determinants of ion permeation in CRAC channels. Proc Natl Acad Sci U S A 106:22516–22521

McNally BA, Prakriya M (2012) Permeation, selectivity, and gating in store-operated CRAC channels. J Physiol 590:4179–4191

McNally BA, Somasundaram A, Yamashita M, Prakriya M (2012) Gated regulation of CRAC channel ion selectivity by STIM1. Nature 482:241–245

McNally BA, Somasundaram A, Jairaman A, Yamashita M, Prakriya M (2013) The C- and N-terminal STIM1 binding sites on Orai1 are required for both trapping and gating CRAC channels. J Physiol 591: 2833–2850

Mercer JC, Dehaven WI, Smyth JT, Wedel B, Boyles RR, Bird GS, Putney JW, Jr. (2006) Large store-operated calcium-selective currents due to co-expression of Orai1 or Orai2 with the intracellular calcium sensor, Stim1. J Biol Chem 281:24979–24990

Mignen O, Thompson JL, Shuttleworth TJ (2008) Orai1 subunit stoichiometry of the mammalian CRAC channel pore. J Physiol 586:419–425

Muik M, Frischauf I, Derler I, Fahrner M, Bergsmann J, Eder P, Schindl R, Hesch C, Polzinger B, Fritsch R, Kahr H, Madl J, Gruber H, Groschner K, Romanin C (2008) Dynamic coupling of the putative coiled-coil domain of ORAI1 with STIM1 mediates ORAI1 channel activation. J Biol Chem 283:8014–8022

Muik M, Fahrner M, Derler I, Schindl R, Bergsmann J, Frischauf I, Groschner K, Romanin C (2009) A Cytosolic Homomerization and a Modulatory Domain within STIM1 C Terminus Determine Coupling to ORAI1 Channels. J Biol Chem 284:8421–8426

Muik M, Fahrner M, Schindl R, Stathopulos P, Frischauf I, Derler I, Plenk P, Lackner B, Groschner K, Ikura M, Romanin C (2011) STIM1 couples to ORAI1 via an intramolecular transition into an extended conformation. Embo J 30:1678–1689

Muik M, Schindl R, Fahrner M, Romanin C (2012) Ca(2+) release-activated Ca(2+) (CRAC) current, structure, and function. Cell Mol Life Sci 69:4163–4176

Mullins FM, Park CY, Dolmetsch RE, Lewis RS (2009) STIM1 and calmodulin interact with Orai1 to induce Ca2+-dependent inactivation of CRAC channels. Proc Natl Acad Sci U S A 106:15495–15500

Oh-hora M, Rao A (2008) Calcium signaling in lymphocytes. Curr Opin Immunol 20:250–258

Palty R, Stanley C, Isacoff EY (2015) Critical role for Orai1 C-terminal domain and TM4 in CRAC channel gating. Cell Res 25:963–980

Palty R, Isacoff EY (2016) Cooperative Binding of Stromal Interaction Molecule 1 (STIM1) to the N and C Termini of Calcium Release-activated Calcium Modulator 1 (Orai1). J Biol Chem 291:334–341

Park CY, Hoover PJ, Mullins FM, Bachhawat P, Covington ED, Raunser S, Walz T, Garcia KC, Dolmetsch RE, Lewis RS (2009) STIM1 clusters and activates CRAC channels via direct binding of a cytosolic domain to Orai1. Cell 136:876–890

Penna A, Demuro A, Yeromin AV, Zhang SL, Safrina O, Parker I, Cahalan MD (2008) The CRAC channel consists of a tetramer formed by Stim-induced dimerization of Orai dimers. Nature 456:116–120

Pozo-Guisado E, Campbell DG, Deak M, Alvarez-Barrientos A, Morrice NA, Alvarez IS, Alessi DR, Martin-Romero FJ (2010) Phosphorylation of STIM1 at ERK1/2 target sites modulates store-operated calcium entry. J Cell Sci 123:3084–3093

Prakriya M, Feske S, Gwack Y, Srikanth S, Rao A, Hogan PG (2006) Orai1 is an essential pore subunit of the CRAC channel. Nature 443:230–233

Putney JW Jr. (1986) A model for receptor-regulated calcium entry. Cell Calcium 7:1–12

Qiao F, Bowie JU (2005) The many faces of SAM. Sci STKE 2005:re7

Roos J, DiGregorio PJ, Yeromin AV, Ohlsen K, Lioudyno M, Zhang S, Safrina O, Kozak JA, Wagner SL, Cahalan MD, Velicelebi G, Stauderman KA (2005) STIM1, an essential and conserved component of store-operated Ca2+ channel function. J Cell Biol 169:435–445

Smyth JT, Petranka JG, Boyles RR, DeHaven WI, Fukushima M, Johnson KL, Williams JG, Putney JW Jr. (2009) Phosphorylation of STIM1 underlies suppression of store-operated calcium entry during mitosis. Nat Cell Biol 11:1465–1472

Soboloff J, Spassova MA, Tang XD, Hewavitharana T, Xu W, Gill DL (2006) Orai1 and STIM reconstitute store-operated calcium channel function. J Biol Chem 281:20661–20665

Spassova MA, Soboloff J, He LP, Xu W, Dziadek MA, Gill DL (2006) STIM1 has a plasma membrane role in the activation of store-operated Ca(2+) channels. Proc Natl Acad Sci U S A 103:4040–4045

Stathopulos PB, Li GY, Plevin MJ, Ames JB, Ikura M (2006) Stored Ca2+ depletion-induced oligomerization of stromal interaction molecule 1 (STIM1) via the EF-SAM region: An initiation mechanism for capacitive Ca2+ entry. J Biol Chem 281:35855–35862

Stathopulos PB, Zheng L, Li GY, Plevin MJ, Ikura M (2008) Structural and mechanistic insights into STIM1-mediated initiation of store-operated calcium entry. Cell 135:110–122

Stathopulos PB, Zheng L, Ikura M (2009) Stromal Interaction Molecule (STIM) 1 and STIM2 Calcium Sensing Regions Exhibit Distinct Unfolding and Oligomerization Kinetics. J Biol Chem 284:728–732

Stathopulos PB, Schindl R, Fahrner M, Zheng L, Gasmi-Seabrook GM, Muik M, Romanin C, Ikura M (2013) STIM1/Orai1 coiled-coil interplay in the regulation of store operated calcium entry. Nature Commun 4:2963

Thompson JL, Shuttleworth TJ (2013) How many Orai's does it take to make a CRAC channel? Sci Rep 3:1961

Tirado-Lee L, Yamashita M, Prakriya M (2015) Conformational Changes in the Orai1 C-Terminus Evoked by STIM1 Binding. PLoS One 10:e0128622

Varnai P, Toth B, Toth DJ, Hunyady L, Balla T (2007) Visualization and manipulation of plasma membrane-endoplasmic reticulum contact sites indicates the presence of additional molecular components within the STIM1-Orai1 Complex. J Biol Chem 282:29678–29690

Vig M, Beck A, Billingsley JM, Lis A, Parvez S, Peinelt C, Koomoa DL, Soboloff J, Gill DL, Fleig A, Kinet JP, Penner R (2006a) CRACM1 multimers form the ion-selective pore of the CRAC channel. Curr Biol 16:2073–2079

Vig M, Peinelt C, Beck A, Koomoa DL, Rabah D, Koblan-Huberson M, Kraft S, Turner H, Fleig A, Penner R, Kinet JP (2006b) CRACM1 is a plasma membrane protein essential for store-operated Ca2+ entry. Science 312:1220–1223

Walsh CM, Chvanov M, Haynes LP, Petersen OH, Tepikin AV, Burgoyne RD (2010) Role of phosphoinositides in STIM1 dynamics and store-operated calcium entry. Biochem J 425:159–168

Williams RT, Manji SS, Parker NJ, Hancock MS, Van Stekelenburg L, Eid JP, Senior PV, Kazenwadel JS, Shandala T, Saint R, Smith PJ, Dziadek MA (2001) Identification and characterization of the STIM (stromal interaction molecule) gene family: coding for a novel class of transmembrane proteins. Biochem J 357:673–685

Williams RT, Senior PV, Van Stekelenburg L, Layton JE, Smith PJ, Dziadek MA (2002) Stromal interaction molecule 1 (STIM1), a transmembrane protein with growth suppressor activity, contains an extracellular SAM domain modified by N-linked glycosylation. Biochim Biophys Acta 1596:131–137

Wu MM, Buchanan J, Luik RM, Lewis RS (2006) Ca2+ store depletion causes STIM1 to accumulate in ER regions closely associated with the plasma membrane. J Cell Biol. 174:803–813

Xu P, Lu J, Li Z, Yu X, Chen L, Xu T (2006) Aggregation of STIM1 underneath the plasma membrane induces clustering of Orai1. Biochem Biophys Res Commun. 350:969–976

Yang X, Jin H, Cai X, Li S, Shen Y (2012) Structural and mechanistic insights into the activation of Stromal interaction molecule 1 (STIM1). Proc Natl Acad Sci U S A 109:5657–5662

Yeromin AV, Zhang SL, Jiang W, Yu Y, Safrina O, Cahalan MD (2006) Molecular identification of the CRAC channel by altered ion selectivity in a mutant of Orai. Nature 443:226–229

Yu F, Sun L, Hubrack S, Selvaraj S, Machaca K (2013) Intramolecular shielding maintains the ER Ca(2)(+) sensor STIM1 in an inactive conformation. J Cell Sci 126:2401–2410

Yuan JP, Zeng W, Dorwart MR, Choi YJ, Worley PF, Muallem S (2009) SOAR and the polybasic STIM1 domains gate and regulate Orai channels. Nat Cell Biol 11:337–343

Zhang SL, Yu Y, Roos J, Kozak JA, Deerinck TJ, Ellisman MH, Stauderman KA, Cahalan MD (2005) STIM1 is a Ca2+ sensor that activates CRAC channels and migrates from the Ca2+ store to the plasma membrane. Nature 437:902–905

Zhang SL, Yeromin AV, Zhang XH, Yu Y, Safrina O, Penna A, Roos J, Stauderman KA, Cahalan MD (2006) Genome-wide RNAi screen of Ca(2+) influx identifies genes that regulate Ca(2+) release-activated Ca(2+) channel activity. Proc Natl Acad Sci U S A 103:9357–9362

Zhang SL, Yeromin AV, Hu J, Amcheslavsky A, Zheng H, Cahalan MD (2011) Mutations in Orai1 transmembrane segment 1 cause STIM1-independent activation of Orai1 channels at glycine 98 and channel closure at arginine 91. Proc Natl Acad Sci U S A 108:17838–17843

Zheng H, Zhou MH, Hu C, Kuo E, Peng X, Hu J, Kuo L, Zhang SL (2013) Differential roles of the C and N termini of Orai1 protein in interacting with stromal interaction molecule 1 (STIM1) for Ca2+ release-activated Ca2+ (CRAC) channel activation. J Biol Chem 288:11263–11272

Zheng L, Stathopulos PB, Li GY, Ikura M (2008) Biophysical characterization of the EF-hand and SAM domain containing Ca2+ sensory region of STIM1 and STIM2. Biochem Biophys Res Commun 369:240–246

Zheng L, Stathopulos PB, Schindl R, Li GY, Romanin C, Ikura M (2011) Auto-inhibitory role of the EF-SAM domain of STIM proteins in store-operated calcium entry. Proc Natl Acad Sci U S A 108:1337–1342

Zhou Y, Mancarella S, Wang Y, Yue C, Ritchie M, Gill DL, Soboloff J (2009) The short N-terminal domains of STIM1 and STIM2 control the activation kinetics of Orai1 channels. J Biol Chem 284:19164–19168

Zhou Y, Meraner P, Kwon HT, Machnes D, Oh-hora M, Zimmer J, Huang Y, Stura A, Rao A, Hogan PG (2010a) STIM1 gates the store-operated calcium channel ORAI1 in vitro. Nat Struct Mol Biol 17:112–116

Zhou Y, Ramachandran S, Oh-Hora M, Rao A, Hogan PG (2010b) Pore architecture of the ORAI1 store-operated calcium channel. Proc Natl Acad Sci U S A 107:4896–4901

Zhou Y, Srinivasan P, Razavi S, Seymour S, Meraner P, Gudlur A, Stathopulos PB, Ikura M, Rao A, Hogan PG (2013) Initial activation of STIM1, the regulator of store-operated calcium entry. Nat Struct Mol Biol 20:973–981